Salidroside Attenuates Cognitive Dysfunction in Senescence-Accelerated Mouse Prone 8 (SAMP8) and Modulating Inflammation on the Gut-brain Axis

Zeping Xie
Traditional Chinese Pharmacological Laboratory, School of Traditional Chinese Medicine, Southern Medical University, Guanghzou https://orcid.org/0000-0002-3120-5565
Hui Lu
School of Traditional Chinese Medicine,Southern Medical University, Guangzhou
Sixia Yang
School of Traditional Chinese Medicine, Southern Medical University, Guangzhou
Yi Zeng
School of Traditional Chinese Medicine, Southern Medical University, Guangzhou
Wei Li
Institute of Chinese Materia Medica, Shanghai University of Traditional Chinese Medicine, Shanghai
Linlin Wang
School of Traditional Chinese Medicine, Southern Medical University, Guangzhou
Guanfeng Luo
School of Traditional Chinese Medicine, Southern Medical University, Guangzhou
Fang Fang
School of Traditional Chinese Medicine, Southern Medical University, Guangzhou
Ting Zeng
School of Traditional Chinese Medicine, Southern Medical University, Guangzhou
Weidong Cheng (chengweidong888@sina.com)

Research

Keywords: Salidroside, cognition, SAMP8; Microglia, Inflammation, microbiota

Posted Date: April 28th, 2020

DOI: https://doi.org/10.21203/rs.3.rs-24799/v1

Abstract

Background Alzheimer's disease (AD), as the most prime cause of dementia, is a fatal neurodegenerative disease characterized by progressive cognitive decline and memory loss. However, A range of therapeutic approaches have shown unsatisfactory outcomes in clinical setting. Thus, it is critical to develop alternative therapies for the treatment of AD. Salidroside(SAL), a herb-derived phenylpropanoid glycoside compound, has been shown to attenuate LPS-induced cognitive impairment. However, the mechanism underlying its neuroprotective effects remains unclear. Here we show a therapeutic effect of SAL in a reliable and stable mouse model of AD, Senescence-Accelerated Mice Prone 8 (SAMP8).

Methods SAMP8 were treated with salidroside, donepezil or saline, cognitive behavioral impairments were assessed using the Morris water maze, Y-maze, and open-field tests. Fecal samples were collected and analyzed by 16S rRNA sequencing, performed on the Illumina MiSEq. Brain samples were analyzed by immunohistochemistry and western blot to detect Beta Amyloid 1–42 deposition. Activation in microglia and neuroinflammatory cytokines was detected by immunofluorescence, Western blot and qPCR. Serum was analyzed by a Mouse High Sensitivity T Cell Magnetic Bead Panel and performed on the Luminex-MAGPIX multiplex immunoassay system.

Results Our results suggested that SAL effectively alleviated hippocampus-dependent memory impairment in SAMP8, and showed no significant difference compared with the donepezil-administration group. SAL significantly (1) reduced toxic beta-amyloid (Abeta) 1–42 deposition; (2) reduced activation of microglia and attenuated proinflammatory factors, IL-1β, IL-6, and TNF-α, in the brain; (3) improved the gut barrier integrity and modified the gut microbiota (reversed the ratio of Bacteroidetes to Firmicutes, and eliminated Clostridiales and Streptococcaceae, which may have been associated with cognitive deficits); and (4) decreased the levels of proinflammatory cytokines in the peripheral circulation, IL-1α, IL-6, IL-17A and IL-12 in particular, according to a multiplex immunoassay.

Conclusion In summary, SAL reversed AD-related changes in SAMP8 potentially through the regulation of the microbiota-gut-brain axis and by modulating inflammation in both peripheral circulation and central nervous system. Our results strongly suggest a therapeutic effect of SAL on cognition-related changes in SAMP8 and highlight its value as a potential source for drug development.

1. Introduction

A prevalence-based study on worldwide costs of dementia has reported an enormous sum of US $818 bn in 2015, with an increase of 35.4% compare to 2010, which related to an increasing number of patients and increasing costs in per person[1]. The latest data from the United States showed that the total costs in 2020 for health care and hospice care for elder people(≥ 65y) with dementia are estimated to be up to $305 billion[2]. Alzheimer's disease (AD), as the most prime cause of dementia, is a fatal neurodegenerative disease characterized by progressive cognitive decline and memory loss. The amyloid cascade hypothesis has been considered the main pathogenic concept in AD research for the last few

decades. It suggests that the accumulation of amyloid-β peptide (Aβ) in the brain tissue is the primary event in AD, followed by the formation of neurofibrillary tangles (NFTs) containing tau protein[3].

Much recent work has revealed the significance of gut microbiota in Alzheimer's disease. The microbiota-gut-brain axis has emerged as a potential key player that can have marked effects on AD pathology[4]. It has been confirmed that germ-free mice exhibited deficit in non-spatial and working memory, indicating a requirement for a commensal microbiota in cognition[5]. It is widely accepted that microbiota have a direct impact on the immune system, as one of the various routes that enable microbiota to communicate with the Central Nervous System (CNS). In addition, microbiota had a profound impact on the maturation of microglial cells and effectively promoted the steady-state condition of microglia via secretion of short-chain fatty acids (SCFA), highlighting an eminent microbiota-gut-brain axis[5, 6]. On the other hand, a growing body of literature has studied immune system-related events in AD recently, which is shown to involve a strong relation with pathogenic and therapeutic relevance [7]. Indeed, the inflammatory reaction occurred in AD is driven mainly by CNS-resident immune cells —microglia in particular, which exerts a dual influence in AD. It is reported that the disruption of its defense function will lead to injury and even death of neurons[8]. Recent evidence strongly implicates the involvement in both the innate and adaptive immune system in AD, and it has been proved that proinflammatory mediators including cytokines, chemokines are increased in the peripheral circulation of individuals with AD [9].

Animal models are paramount in AD research, especially when linking pathological changes, such as Aβ and tau accumulation. The senescence-accelerated mouse prone 8 (SAMP8), a spontaneous model of dementia, exhibits deficit in learning and memory abilities as well as pathological alterations in the brain, including increased oxidative stress, inflammation, Aβ accumulation and tau hyperphosphorylation[10]. In contrast, its control, Senescence Accelerated Mouse Resistant 1(SAMR1), ages normally. Salidroside(SAL), a herb-derived phenylpropanoid glycoside compound, has been shown to attenuate cognitive impairment in both LPS-induced and d-gal-induced cognitive deficits models[11, 12]. Recent evidence reveals that Salidroside provided neuroprotection by modulating mitochondrial biogenesis and microglial polarization[13, 14]. Notably, Salidroside exhibits significant anti-inflammatory effects in multiple diseases such as osteoarthritis[15], Colitis[16], Skeletal muscle atrophy[17], renal interstitial fibrosis, [18] and CNS diseases like as well[14, 19]. Furthermore, recent findings have suggested salidroside alleviated liver injury induced by maintaining the balance of gut microbiota[20]. Thus, it is reasonable to speculate that salidroside provided its neuroprotective function by regulating gut microbiota and systemic inflammation, and subsequently involving neuropathologic changes. This study reports that salidroside ameliorates cognitive decline in a reliable AD model, SAMP8, and its beneficial effects on inflammation-related microbiota-gut-brain axis.

2. Material And Methods

2.1 Animals

There were 10 male SAMR1 mice and 30 male SAMP8, with a body mass of 27–32 g. They were obtained from the First Affiliated Hospital of Tianjin Traditional Chinese Medicine University (Tianjin, China). The mice were housed in the SPF level laboratory in Southern Medical University (Guangzhou, China) under standard conditions (22–23 °C, 12-h light/dark cycle, and 60% ± 10% humidity) and provided with water and food ad libitum. They were adapted to their environmental conditions for 7 days before experiments.

2.2 Experimental Designs

After acclimatization to laboratory conditions for 1 week, 10 male SAMR1 were defined as the control group(R1-Ct, treated with saline), and 30 SAMP8 were randomly divided into three groups (10 /group): model group(P8-Ct, treated with saline), salidroside group(P8-SAL, treated with 50mg·kg^{-1}·d^{-1} salidroside) and donepezil group(P8-DNP, treated with 1mg·kg^{-1}·d^{-1} donepezil). Salidroside($C_{14}H_{20}O_{7,}$ purity > 98%) was obtained from Macklin Biochemical Co., Ltd (Shanghai, China). Donepezil was supplied by Eisai Pharmaceutical Co., Ltd. (Tokyo, Japan). All the mice were treated once per day for 3 months and tissues were then removed for other experiments. Every effort to minimize suffering was made.

2.3 Open Fields Test (oft)

Spontaneous activity was tested in a clear plastic cube box (40 × 40 × 40 cm) under a camera. Each mouse was placed in the center of the Open Field and given 5 min to move freely. Total traveled distances were analyzed using Smart V3.0 Panlab software.

2.4 Y-maze

Spontaneous spatial recognition was assessed in a Y maze apparatus, which was composed of three identical arms (30 cm length, 8 cm width, and 15 cm height). Each mouse was allowed to explore the three arms freely from the center of the maze for 5 min. The sequence of arm entries was recorded by a camera right above the apparatus. A spontaneous alternation was defined as arm choices differing from the previous two choices (e.g., ABC, BCA, CAB, etc). Alternation percentage (%) was calculated as a proportion of total spontaneous alternations to possible alternations (total arm entries − 2) × 100%.

2.5 Morris Water Maze (mwm)

To assess the ability of hippocampus-dependent learning and memory ability of the mice, the Morris Water Maze test was performed after the Y maze, The MWM apparatus consists of a blue circular pool of 120 cm in diameter with *2/3 of* water(25℃±1) containing nontoxic ink, and a circular platform (14 cm in diameter) submerged 1.5 cm below the water surface. The MWM tests were performed as described

previously[21]. Briefly, during the acquisition trial (days 1–5), each mouse was trained to find the hidden platform within 60 s. The searching trajectories were monitored with a camera and the escape latencies were measured using DigBehv-Morris software (Shanghai Jiliang, China). Within 60 s, the time each mouse spends finding the platform was defined as the escape latency. If the mouse did not find the platform successfully, the latency was recorded as 60 s, and it was gently guided to the platform and allowed to stay on the platform for 10 s. A probe trial was performed on day 6 with the platform removed. The number of target platform crossings and the time spent in target in each quadrant were recorded.

2.6 Histological Analysis

Mice were anesthetized and intracardially perfused with cold PBS. The brain and intestine tissues were carefully dissected and immersed in 4% paraformaldehyde at 4 °C overnight. After paraffin-embedded, the tissues were cut into sections. Intestine tissue was performed by hematoxylin-eosin (HE) staining. Immunohistochemistry (IHC) analysis was performed on the brain sections with Beta Amyloid 1–42 antibody (ab201060-10, 1:1000; Abcam) following the standard IHC-paraffin protocol from Abcam. Pictures were taken with a MVX10 microscope (Olympus). For immunofluorescence(IF) analysis, the brain sections were blocked with 5% BSA for 1 h and incubated with primary antibodies,CD68 (1:500; Servicebio), overnight at 4 °C, followed by incubation with anti-rabbit Cy3-labeled secondary antibody for 1 h at room temperature. The nuclei were stained with DAPI reagent (Servicebio). For IF imaging, confocal microscopy (Zeiss, LSM800) was used and images were taken and processed with the ZEN software and Microsoft PowerPoint.

2.7 Flow Cytometry

Flow cytometry was performed to detect the proportion of CD4 or CD8 positive lymphocytes in the spleen. Subsequent to sacrifice, the spleen was removed in sterile conditions, weighed, and processed into a single cell suspension, which then stained according to standard protocols for flow cytometry with the following antibodies: CD3 (BD Biosciences, 560527), CD4 (BD Biosciences, 562891), CD8a (BD Biosciences, 553030). Labeled cells were fixed with 1% PFA and analyzed with a LSRFortessa X-20 flow cytometer (BD Biosciences, MA, USA) on FACSDiva 8.0.1 software (BD Biosciences, MA, USA). In each sample, the corresponding isotype control antibodies were used. CD3 + cells were gated as T lymphocytes, and then the CD4 + and CD8 + populations were analyzed.

2.8 Western Blot

Protein was extracted using a Whole Cell Lysis Assay (KeyGEN, Nanjing, China) according to the manufacturer's instructions. The protein was separated using SDS-PAGE and transferred to PVDF membranes (Millipore, Bedford, MA, USA). The membranes were blocked in 5% BSA for 1.5 h and then incubated with the following primary antibodies: Anti-beta Amyloid 1–42 (ab201060-10, 1:1000; Abcam),

occludin (DF7504, 1:1000; Affinity), ZO-1 (AF5145; 1:1000; Affinity), β-Actin(4970; 1:1000; CST), GAPDH-HRP (HRP-60004, 1:8000; Proteintech).after washed with TBS-T, the membranes were incubated with secondary antibodies(SA00001-2, 1:8000; Proteintech), except for GAPDH-HRP, for 2 h at 4℃. The protein signals were detected using an ECL system (Affinity, Jiangsu, China).

2.9 PCR

Total RNA was extracted from brain tissues using Trizol reagent (Vazyme Biotech Co., Ltd) and converted to cDNA using HiScript® III RT SuperMix for qPCR (+ gDNA wiper) kit (Vazyme Biotech Co., Ltd). qPCR reactions were performed with ChamQ Universal SYBR qPCR Master Mix (Vazyme Biotech Co., Ltd). All primers used are shown in **(Table S1)**. The relative quantitative calculation of of mRNA was normalized in relevance to that of GAPDH (B661304, Sangon Biotech, Shanghai, China). The relative expression of genes was analyzed by the method of fold changes($2^{-\Delta\Delta Ct}$).

2.10 16s Rrna Sequencing And Data Analysis Of Fecal Sample

Fecal samples were collected by standardized collection procedures and were chosen at random, and a final n = 5/group was used for 16S rRNA sequencing. DNA samples were quantified, followed by the amplification of the V3-V4 hypervariable region using the 338F(5'ACTCCTACGGGAGGCAGCAG 3') and 806R(5'GGACTACHVGGGTWTCTAAT 3') primers. ALL PCR amplicons were concentrated and purified by gel electrophoresis, and subsequently extracted to obtain 3 μg of amplicons. Sequencing was performed on the Illumina MiSeq.

2.11 Multiplex Cytokine Assay

Serum was collected by centrifugation at 1000xg for 15 min at 4 °C, aliquoted, and stored at -80 °C until analysis. Mouse High Sensitivity T Cell Magnetic Bead Panel ((EMD Millipore, Billerica, MA, USA) was performed on the Luminex-MAGPIX multiplex immunoassay system according to the manufacturer's instructions. Data were analyzed using Milliplex Analyst 5.1 software (EMD Millipore, Billerica, MA, USA).

2.12 Statistical Analyses

The statistical analyses were performed with SPSS (IBM SPSS Statistics for Windows, version 20; IBM Corp., Armonk, NY, USA). Comparisons between groups were performed using one-way ANOVA, followed by LSD or Dunnett's T3 post hoc test. The following significance levels were used for comparisons between independent groups: $^{\#}P < 0.05$, $^{\#\#}P < 0.01$, $^{\#\#\#}P < 0.001$ versus R1-Ct group; $^{*}P < 0.05$, $^{**}P < 0.01$, $^{***}P < 0.001$ versus P8-Ct group, and "ns" indicates no significant difference.

3. Results

3.1 Effect of SAL on the behavioral performance of SAMP8

we treated mice with 50mg·kg^{-1}·d^{-1} of SAL, 1mg·kg^{-1}·d^{-1} of Donepezil or saline for 3 months, as described in Materials and Methods. The treatment was started when mice were 5 months of age, when AD pathological changes began to emerge in this mouse strain[22]. To evaluate the effect of salidroside on the behavioral performance of SAMP8, the Open Field Test (OFT) was conducted on day60 and followed by Y maze test. Afterward, the Morris Water Maze (MWM) was performed for six days. Subsequently, the mice were sacrificed by euthanasia for histological and biochemical analyses (Fig. 1A). The learning trials in MWM revealed that SAMP8 took longer latencies to a hidden platform than SAMR1, and the latencies are shortened by treatment with SAL or DNP (Fig. 1B-C). Moreover, SAL treatment yields a significant improvement in the impaired rate of time and the number of crossings in the target quadrant for memory recall during a 60 sec probe trial on the last day of MWM. Although P8-DNP showed a little better performance than that of P8-SAL, there was no statistical difference ($p > 0.05$). (Fig. 1D-E). In the Y maze, SAMP8 treated with SAL and DNP also showed a significantly higher correct alternation rate than the model group (Fig. 1F). We further examined the spontaneous locomotor and exploratory behaviors of these mice in the open field test. Consistent with previous findings[23], SAMP8 traveled a longer distance in the open field than SAMR1. However, SAL treatment has the same high autonomy as the model group(Fig. 1G). These observations suggest that SAL alleviated hippocampus-dependent memory impairment in SAMP8, but may not change its anxiety-like behavior.

3.2 Effect Of Sal On Neurodegeneration And Neuroinflammation In Samp8

The immunohistochemical results showed the amyloid-β peptide 1–42($A\beta_{1-42}$) was significantly expressed in the hippocampus (CA1 and CA3 regions) and cortex in SAMP8, which was almost negative in SAMR1. Due to its exposed hydrophobic surface area, monomers or oligomers of $A\beta_{1-42}$ tend to combine the membrane of neurons and cause toxicity[24]. However, SAL administration reduced the neuronal damage from $A\beta_{1-42}$ in SAMP8, which is considered to lead to an improvement in cognitive function (Fig. 2A). We observed a strong CD68 immunoreactivity in the P8-Ct, and a decreased number of CD68-positive cells in P8-SAL group(Fig. 2A), indicated that SAL reduces microglial activation in SAMP8 (Fig. 2B). Consistently, the mRNA expression of the Amyloid Precursor Protein(APP), CD68 and ionized calcium binding adaptor molecule 1 (IBA-1) were also prevented by SAL. Moreover, The production of proinflammatory cytokines (IL-1β, IL-6, TNF-α) was decreased by SAL (Fig. 2C). Western-blot analysis yielded consistent results with the IHC for $A\beta_{1-42}$ (Fig. 2D). Our data revealed that SAL administration significantly reduced toxic amyloid-β peptide deposition in SAMP8, accompanied by a reduction in microglial neuroinflammation.

3.3 Effect of SAL on intestinal barrier and gut microbiota in SAMP8

Histological analysis and western blot analysis demonstrated the integrity and the tight junction of the intestine was destroyed in SAMP8. In the P8-SAL group, the structure of the intestinal mucosa was more complete, with less inflammatory infiltration in crypt and less swelling of villi, and conferred higher ZO-1 and occludin protein levels **(**Fig. 3A-B**)**.

The sequence of the 16S rRNA gene V3/V4 variable region from the feces sample was analyzed. To evaluate alterations in the microbial alpha diversity, we measured Chao, Shannon, simpson, sob and ace diversity indices, which showed no significant differences among groups**(Table S2)**. Principal coordinates analysis (PCoA) revealed that the cluster from P8-SAL samples was more similar to that of R1-Ct, whereas the P8-Ct cluster was more distinct **(**Fig. 3C**)**.

To illustrate the differences in the microbiota composition, we conducted heatmap, bar plot, and Circos analyses. At the phylum level, there is a decrease in the Bacteroidetes phyla(R1-Ct: P8-Ct: P8-SAL = 34%: 30%: 36%) and an increase in Firmicutes phyla(30%: 40%: 29%) in P8-Ct, which is considered an age-related difference that may also be associated with altered immune system function[25]. Interestingly, SAL treatment reversed the ratio of Bacteroidetes to Firmicutes, which was more similar to that of R1-Ct **(**Fig. 3F**)**. Community barplot analysis at genus level showed that SAL administration increased the median abundance of Norank_f_Muribaculaceae(R1-Ct: P8-Ct: P8-SAL = 37%: 26%: 37%), alloprevotella(70%: 0.0%: 30%) and parasutterella(48%: 6.3%: 46%), and decreased the median abundance of prevotellaceae(32%: 37%: 31%), Lachnospiraceae_NK4A136_group(30%: 46%: 24%), Unclassified_f_Lachnospiraceae(35%: 42%: 23%), Alistipes(28%: 38%: 34%), Norank_f_Lachnospiraceae(26%: 44%: 29%), Odoribacter(17%: 55%: 28%), Rikenellaceae_RC9_gut_group(14%: 61%: 25%), Ruminococcaceae_UCG-014(5.1%: 78%: 17%) and Ruminiclostridium_9(28%: 47%: 25%) in SAMP8**(**Fig. 3D**)**. Circos diagram was used to visualize the association between abundance relationship between samples and bacterial communities on the genus level, which consistent with the bar plot analysis results **(**Fig. 3E**)**. To further identify specific individual bacterial taxa that differentially enriched among groups, we applied the LEfSe analysis**(Figure S1)**. As shown below, a significant enrichment in 2 families (Clostridiales_vadinBB60, Streptococcaceae), 4 genera (norank_f_Clostridiales_vadinBB60, Peptococcus, Streptococcus, Ruminococcaceae_UCG_009) and 7 Species were identified in SAMP8, which were eliminated by SAL administration, accompanied by five newborn species present only in P8-SAL **(**Fig. 3G**)**.

3.4 Effect Of Sal On Systematic Inflammation In Samp8

To assessed the effects of SAL on peripheral cytokine secretion, a magnetic bead analysis approach was used to detect the concentration of 18 cytokines/chemokines in the plasma. Results showed that GM-CSF, IL-1α, IL-6, IL-12, IL-13, and IL-17A increased in SAMP8**(Figure S2)**, among which the levels of IL-1α

(Fig. 4B), IL-6(Fig. 4C), IL-17A(Fig. 4D) and IL-12(Fig. 4E) were decreased after SAL administration. These data suggested that there is chronic inflammation in the circulation of SAMP8, and SAL has significant anti-inflammatory properties in SAMP8. In addition, the flow cytometric results demonstrated that the number of $CD3^+CD4^+$ lymphocytes and the $CD4^+/CD8^+$ ratio were significantly increased in the spleen of SAMP8. However, there is no statistical significance after SAL administration(Fig. 4F).

4. Discussion

Senescence-Accelerated Prone 8 mouse (SAMP8) is considered a reliable experimental model for studying the pathogenesis and developing preventive and therapeutic strategies for age-related AD[26]. SAMP8 develops early deficits in learning and memory (5 months) accompanied with a number of AD-related brain alterations, including increased oxidative stress and tau phosphorylation[22]. Here we treated 5-month-old SAMP8 with salidroside for 3 months. At 8 months of age, the mice already presented a rather strong AD-related phenotype compared to SAMR1, while the curative effect of salidroside has also become prominent. Our results suggested that SAL effectively alleviated hippocampus-dependent memory impairment in SAMP8 and showed no significant difference compared with the donepezil-administration group. Though donepezil exerts a neuroprotective effect and is widely used in the treatment of AD, numerous studies have demonstrated that it causes adverse events including symptoms such as hostility, somnolence, fecal incontinence, nausea and rhinitis[27–29]. Previous studies have shown that salidroside exerts neuroprotection and no significant adverse effects were reported until now. Thus, salidroside has the potential to develop into an alternative treatment for AD.

In this study, salidroside was shown to effectively attenuate both $A\beta_{1-42}$ deposition and neuroinflammation in the brain of SAMP8. Based on a 3D non-cell-autonomous cell culture model, the latest research showed that high Aβ42/40 ratio drives robust tau phosphorylation in human neurons, suggested that selectively reducing Aβ42/40 ratio could be a novel therapeutic approach[30]. In the present study, less $A\beta_{1-42}$ deposition and neuron death were observed in the hippocampus (CA1 and CA3 regions) and cortex of SAMP8 after salidroside treatment, confirming its therapeutic efficacy. Indeed, Oligomers of $A\beta_{1-42}$ have a high tendency to attach to the membrane and have been implicated in neuron injury and cognitive impairment associated with Alzheimer's disease[31]. Pro-inflammatory microglial activities are believed to result in various detrimental effects on the brain and contribute to neurodegeneration. Especially, the activation of microglia increases the formation of Aβ oligomers and further aggregation[24, 32]. We showed here that the number of activated microglia cells, determined by CD68 immunofluorescence, was significantly reduced in salidroside-treated SAMP8. Moreover, the mRNA levels of pro-inflammatory cytokines, IL-1β, IL-6, and TNF-α, decreased by varying degrees in SAMP8 brain after salidroside administration. These results therefore illustrated a novel effect of salidroside through attenuating neuroinflammation in the AD brain.

Multiple researches indicate that microbial colonization of the gut is linked to dementia pathogenesis via detrimental effects on metabolic disorders or low-grade inflammation progress, leading to damage to the

brain[33]. Consistent with previous studies[34], our findings provided further evidence that the microbiota–gut–brain axis may be involved in AD-like pathogenesis in SAMP8. PCoA and microbiota composition analysis revealed that the cluster from salidroside-treated SAMP8 was more similar to that of SAMR1, whereas the cluster from untreated SAMP8 was the most distinct. In our study, shifts in the ratio of Bacteroidetes to Firmicutes were observed in SAMP8, which is one of the classic age-related change in microbiota composition that is associated with increased inflammation [25, 35]. The reversal effect of salidroside indicated its potential for delaying senescence and reducing inflammation. A significant enrichment in 2 families (Clostridiales_vadinBB60, Streptococcaceae), 4 genera (norank_f_Clostridiales_vadinBB60, Peptococcus, Streptococcus, Ruminococcaceae_UCG_009) and 7 Species were identified in SAMP8, which were eliminated by salidroside administration. These suggested an effect of salidroside on normalizing the alterations of the intestinal microbiota. It should be noted that Clostridiales and Streptococcaceae are classified as firmicutes and may have been associated with cognition[36]. In addition, five newborn species present only in P8-SAL are accompanied, and whether they are beneficial or not requires further study to explain.

Given the importance of microglial functions in the promotion of neurodegenerative processes, it is reasonable to speculate that the changes in gut microbiota, which are capable of inducing inflammation via some cell components or metabolites, may influence these inflammatory and degenerative alterations in the AD brain. In our results, salidroside was able to restore intestinal barrier integrity, which may result in less accumulation of microbial products in the peripheral as well as reduction of chronic inflammation. As immune-related effect in bacteria is an important step toward understanding bacterial contributions to cognition, we estimated alterations of pro-inflammatory and anti-inflammatory cytokines/ chemokines in circulating levels, which directly affect brain function. Low-grade systemic inflammation was observed in the serum of SAMP8, whereas salidroside was able to decreased the levels of proinflammatory cytokines, IL-1α, IL-6, IL-17A and IL-12. Notably, the elevated levels of these four proinflammatory cytokines are reported to be involved in the subsequent cognitive decline or pathology of AD[37–40]. Primarily based on murine models, Th1 cells significantly accelerates markers of Alzheimer's disease[41], and Th17 cells have also been described to induced severe fluctuation in neuronal intracellular Ca(2+) concentration, causing neuronal damage and neuroinflammation in vivo imaging experiments[42]. It is known that IL-12 induces T-lymphocytes to differentiate into Th1, while IL-17A is a Th17-specific cytokine, and the pleiotropic cytokine IL-6 is also crucial to the differentiation of Th17 cells. Indeed, there is interactions between serum profiles of inflammatory factors and gut microbiomes. One study suggested the variability of the microbiota exhibited positive correlation with IL-6, especially the phylum Proteobacteria[43]. Moreover, It has been reported that the blocking of IL-1α led to a modification in gut microbiome and effectively reduced inflammation and damage in a mice model of Crohn's-like ileitis[44]. And microbial products have direct effects on the immune system, which affects brain function through cytokines in the circulating levels[45]. It has been reported that many of the bacterial benefits on learning and memory occur alongside reductions in proinflammatory cytokines[46–48]. One study showed that systemic immune alterations triggered and drove the development of AD-related neuropathology comprising Aβ

accumulation and tau phosphorylation, microglia and gliosis activation in wild-type mice, suggesting that immune reactions can precede AD-related pathology and may even be sufficient to cause it[49]. Thus, The effect of salidroside on cognition may be associated with the recovered changes of gut microbiota composition, which is crucial for the reduction of peripheral low-grade inflammation, resulting in improvement of the brain-blood barrier function and neuroinflammatory stimuli suppression.

5. Conclusion

SAL reversed AD-related changes in SAMP8 potentially through the regulation of the microbiota-gut-brain axis and by modulating inflammation in both peripheral circulation and central nervous system. Our results strongly suggest a therapeutic effect of SAL on cognition-related changes in SAMP8 and highlight its value as a potential source for drug development.

6. Abbreviations

AD
alzheimer's disease; SAL:salidroside; SAMP8:Senescence-Accelerated Mice Prone 8; Aβ:amyloid- β peptide; NFTs:neurofibrillary tangles; CNS:central nervous system; SCFA:short-chain fatty acids; SAMR1:Senescence-Accelerated Mice Resistant 1; OFT:open field test; MWM:Morris water maze; HE:hematoxylin-eosin; IHC:immunohistochemistry; IF:immunofluorescence; IBA-1:ionized calcium binding adaptor molecule 1; APP:Amyloid Precursor Protein; IL:Interleukin; PCOA:Principal coordinates analysis; Th:helper T cell; GM-CSF:Granulocyte-macrophage Colony Stimulating Factor.

7. Declarations

7.1 Ethical Approval and Consent to participate

All experimental protocols and animal handling procedures were conducted in strict accordance with the Guide for the Care and Use of Laboratory Animals, published by the National Institutes of Health (NIH Publications No. 8023, revised in 1978). This study was approved by the Ethical Committee on Animal Experimentation of the Southern Medical University.

7.2 Consent for publication

Not applicable.

7.3 Availability of supporting data

All data generated or analysed during this study are included in this published article and its supplementary information files.

7.4 Competing interests

The authors declare no competing interests.

7.5 Funding

This research was funded by the Science and Technology Program of Guangzhou(grant number: 201904010168) , National Natural Science Foundation of China (grant number: 81973641), and National Key Research and Development Program of China (grant number: 2018YFC1704404).

7.6 Authors' contributions

Xie designed and performed experiments, analyzed the data, and drafted the manuscript. Lu collected the fecal samples and assisted with the 16S rRNA sequencing analysis. Yang, ZY, Fang and ZT assisted with the histological staining and qPCR. Li designed the flow cytometry experiment and assisted with flow cytometry data acquisition and analysis. Wang and Luo assisted behavioral tests and western blot. Fang assisted with multiplex immunoassay experiments. Cheng provided study supervision and manuscript revision. The authors read and approved the final manuscript.

7.7 Acknowledgements

We sincerely thank prof. Xingmei Zhang and prof. Yuyao Chen, and the help from the Department of Neurobiology, Southern Medical University.

References

1. The worldwide costs of dementia 2015 and comparisons with 2010 [J]
   WIMO A, GUERCHET M, ALI G C, et al. The worldwide costs of dementia 2015 and comparisons with 2010 [J]. Alzheimer's dementia: the journal of the Alzheimer's Association, 2017, 13(1): 1–7.
2. 2020 Alzheimer's disease facts and figures [J]. Alzheimer's & dementia: the journal of the Alzheimer's Association, 2020.
3. HARDY J, SELKOE D J. The amyloid hypothesis of Alzheimer's disease: progress and problems on the road to therapeutics [J]. Science (New York, NY), 2002, 297(5580): 353-6.
4. CRYAN JF, O'RIORDAN K J, COWAN C S M, et al. The Microbiota-Gut-Brain Axis [J]. Physiological reviews. 2019;99(4):1877–2013.
5. THION MS, LOW D, SILVIN A, et al. Microbiome Influences Prenatal and Adult Microglia in a Sex-Specific Manner [J]. Cell. 2018;172(3):500 – 16.e16.

6. ERNY D, HRABE DE ANGELIS A L, JAITIN D, et al. Host microbiota constantly control maturation and function of microglia in the CNS [J]. Nature neuroscience. 2015;18(7):965–77.
7. HEPPNER F L, RANSOHOFF R M BECHERB. Immune attack: the role of inflammation in Alzheimer disease [J]. Nature reviews Neuroscience. 2015;16(6):358–72.
8. HICKMAN S, IZZY S, SEN P, et al. Microglia in neurodegeneration [J]. Nature neuroscience. 2018;21(10):1359–69.
9. CAO W, ZHENG H. Peripheral immune system in aging and Alzheimer's disease [J]. Molecular neurodegeneration. 2018;13(1):51.
10. CURRAIS A, GOLDBERG J, FARROKHI C, et al. A comprehensive multiomics approach toward understanding the relationship between aging and dementia [J]. Aging. 2015;7(11):937–55.
11. XU N, HUANG F, JIAN C, et al. Neuroprotective effect of salidroside against central nervous system inflammation-induced cognitive deficits: A pivotal role of sirtuin 1-dependent Nrf-2/HO-1/NF-kappaB pathway [J]. Phytother Res, 2019, 33(5): 1438–47.
12. GAO J, HE H, JIANG W, et al. Salidroside ameliorates cognitive impairment in a d-galactose-induced rat model of Alzheimer's disease [J]. Behav Brain Res. 2015;293:27–33.
13. BARHWAL K, DAS S K, KUMAR A, et al. Insulin receptor A and Sirtuin 1 synergistically improve learning and spatial memory following chronic salidroside treatment during hypoxia [J]. Journal of neurochemistry. 2015;135(2):332–46.
14. LIU X, WEN S, YAN F, et al. Salidroside provides neuroprotection by modulating microglial polarization after cerebral ischemia [J]. J Neuroinflamm. 2018;15(1):39.
15. CHEN D, LU D, LIU H, et al. Pharmacological blockade of PCAF ameliorates osteoarthritis development via dual inhibition of TNF-alpha-driven inflammation and ER stress [J]. EBioMedicine. 2019;50:395–407.
16. LIU J, CAI J, FAN P, et al. The Abilities of Salidroside on Ameliorating Inflammation, Skewing the Imbalanced Nucleotide Oligomerization Domain-Like Receptor Family Pyrin Domain Containing 3/Autophagy, and Maintaining Intestinal Barrier Are Profitable in Colitis [J]. Frontiers in pharmacology, 2019, 10(1385.
17. HUANG Z, FANG Q, MA W, et al. Skeletal Muscle Atrophy Was Alleviated by Salidroside Through Suppressing Oxidative Stress and Inflammation During Denervation [J]. Frontiers in pharmacology, 2019, 10(997.
18. LI R, GUO Y, ZHANG Y, et al. Salidroside Ameliorates Renal Interstitial Fibrosis by Inhibiting the TLR4/NF-kappaB and MAPK Signaling Pathways [J]. International journal of molecular sciences, 2019, 20(5).
19. WANG C, WANG Q, LOU Y, et al. Salidroside attenuates neuroinflammation and improves functional recovery after spinal cord injury through microglia polarization regulation [J]. J Cell Mol Med. 2018;22(2):1148–66.
20. YUAN Y, WU X, ZHANG X, et al. Ameliorative effect of salidroside from Rhodiola Rosea L. on the gut microbiota subject to furan-induced liver injury in a mouse model [J]. Food and chemical toxicology:

an international journal published for the British Industrial Biological Research Association, 2019, 125(333 – 40.

21. O'NEAL-MOFFITT G DELICV, BRADSHAW P C, et al. Prophylactic melatonin significantly reduces Alzheimer's neuropathology and associated cognitive deficits independent of antioxidant pathways in AbetaPP(swe)/PS1 mice [J]. Molecular neurodegeneration, 2015, 10(27.
22. PALLAS M, CAMINS A, SMITH M A, et al. From aging to Alzheimer's disease: unveiling "the switch" with the senescence-accelerated mouse model (SAMP8) [J]. Journal of Alzheimer's disease: JAD. 2008;15(4):615–24.
23. YANAI S, ENDO S. Early onset of behavioral alterations in senescence-accelerated mouse prone 8 (SAMP8) [J]. Behavioural brain research, 2016, 308(187 – 95.
24. NARAYAN P, GANZINGER K A, MCCOLL J, et al. Single molecule characterization of the interactions between amyloid-beta peptides and the membranes of hippocampal cells [J]. J Am Chem Soc. 2013;135(4):1491–8.
25. NICHOLSON JK, HOLMES E, KINROSS J, et al. Host-gut microbiota metabolic interactions [J]. Science (New York, NY), 2012, 336(6086): 1262-7.
26. CHENG X R, ZHOU W X, ZHANG Y X. The behavioral, pathological and therapeutic features of the senescence-accelerated mouse prone 8 strain as an Alzheimer's disease animal model [J]. Ageing Res Rev. 2014;13:13–37.
27. ADLIMOGHADDAM A, NEUENDORFF M, ROY B, et al. A review of clinical treatment considerations of donepezil in severe Alzheimer's disease [J]. CNS neuroscience & therapeutics, 2018, 24(10): 876 – 88.
28. LEE C, LEE K, YU H, et al. Adverse Events With Sustained-Release Donepezil in Alzheimer Disease: Relation to Body Mass Index [J]. J Clin Psychopharmacol. 2017;37(4):401–4.
29. BIRKS J, HARVEY RJ. Donepezil for dementia due to Alzheimer's disease [J]. The Cochrane database of systematic reviews, 2006, 1): Cd001190.
30. KWAK SS, WASHICOSKY K J BRANDE, et al. Amyloid-beta42/40 ratio drives tau pathology in 3D human neural cell culture models of Alzheimer's disease [J]. Nature communications. 2020;11(1):1377.
31. GUGLIELMOTTO M, MONTELEONE D, PIRAS A, et al. Abeta1-42 monomers or oligomers have different effects on autophagy and apoptosis [J]. Autophagy. 2014;10(10):1827–43.
32. VENEGAS C, KUMAR S, FRANKLIN B S, et al. Microglia-derived ASC specks cross-seed amyloid-beta in Alzheimer's disease [J]. Nature. 2017;552(7685):355–61.
33. ALKASIR R, LI J, LI X, et al. Human gut microbiota: the links with dementia development [J]. Protein cell. 2017;8(2):90–102.
34. PENG W, YI P, YANG J, et al. Association of gut microbiota composition and function with a senescence-accelerated mouse model of Alzheimer's Disease using 16S rRNA gene and metagenomic sequencing analysis [J]. Aging. 2018;10(12):4054–65.

35. COWAN T E, PALMNAS M S, YANG J, et al. Chronic coffee consumption in the diet-induced obese rat: impact on gut microbiota and serum metabolomics [J]. J Nutr Biochem. 2014;25(4):489–95.
36. BAJAJ JS, SALZMAN N H, ACHARYA C, et al. Fecal Microbial Transplant Capsules Are Safe in Hepatic Encephalopathy: A Phase 1, Randomized, Placebo-Controlled Trial [J]. Hepatology. 2019;70(5):1690–703.
37. VEERHUIS R, VAN BREEMEN M J, HOOZEMANS JM, et al. Amyloid beta plaque-associated proteins C1q and SAP enhance the Abeta1-42 peptide-induced cytokine secretion by adult human microglia in vitro [J]. Acta Neuropathol. 2003;105(2):135–44.
38. ITALIANI P, PUXEDDU I. NAPOLETANO S, et al. Circulating levels of IL-1 family cytokines and receptors in Alzheimer's disease: new markers of disease progression? [J]. J Neuroinflamm. 2018;15(1):342.
39. FRAGOULIS A, SIEGL S, FENDT M, et al. Oral administration of methysticin improves cognitive deficits in a mouse model of Alzheimer's disease [J]. Redox biology, 2017, 12(843 – 53.
40. VOM BERG J, MILLER K R PROKOPS, et al. Inhibition of IL-12/IL-23 signaling reduces Alzheimer's disease-like pathology and cognitive decline [J]. Nature medicine. 2012;18(12):1812–9.
41. LAMBRACHT-WASHINGTON D, QU B X FUM, et al. DNA immunization against amyloid beta 42 has high potential as safe therapy for Alzheimer's disease as it diminishes antigen-specific Th1 and Th17 cell proliferation [J]. Cell Mol Neurobiol. 2011;31(6):867–74.
42. SIFFRIN V, RADBRUCH H, GLUMM R, et al. In vivo imaging of partially reversible th17 cell-induced neuronal dysfunction in the course of encephalomyelitis [J]. Immunity. 2010;33(3):424–36.
43. BIAGI E, NYLUND L, CANDELA M, et al. Through ageing, and beyond: gut microbiota and inflammatory status in seniors and centenarians [J]. PloS one. 2010;5(5):e10667.
44. MENGHINI P, CORRIDONI D, BUTTO L F, et al. Neutralization of IL-1alpha ameliorates Crohn's disease-like ileitis by functional alterations of the gut microbiome [J]. Proceedings of the National Academy of Sciences of the United States of America, 2019.
45. CRYAN JF, DINAN TG. Mind-altering microorganisms: the impact of the gut microbiota on brain and behaviour [J]. Nature reviews Neuroscience. 2012;13(10):701–12.
46. BUROKAS A, ARBOLEYA S, MOLONEY R D, et al. Targeting the Microbiota-Gut-Brain Axis: Prebiotics Have Anxiolytic and Antidepressant-like Effects and Reverse the Impact of Chronic Stress in Mice [J]. Biol Psychiatry. 2017;82(7):472–87.
47. ALLEN A P, HUTCH W, BORRE Y E, et al. Bifidobacterium longum 1714 as a translational psychobiotic: modulation of stress, electrophysiology and neurocognition in healthy volunteers [J]. Translational psychiatry. 2016;6(11):e939.
48. WANG T, HU X. LIANG S, et al. Lactobacillus fermentum NS9 restores the antibiotic induced physiological and psychological abnormalities in rats [J]. Beneficial microbes. 2015;6(5):707–17.
49. KRSTIC D, MADHUSUDAN A, DOEHNER J, et al. Systemic immune challenges trigger and drive Alzheimer-like neuropathology in mice [J]. Journal of neuroinflammation, 2012, 9(151.

Figures

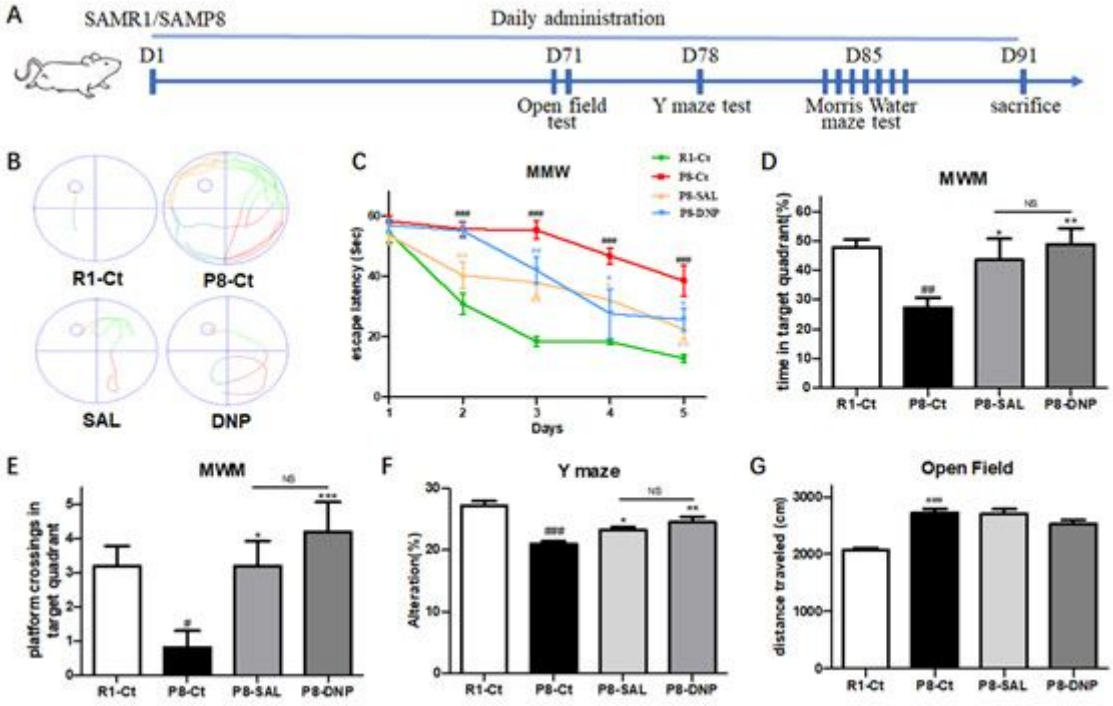

Figure 1

Effect of SAL on the behavioral performance of SAMP8. (A)Scheme of experimental design. (B) representative automated traces from day 5 in MWM are shown for each group. (C) escape latency to get to the unvisible platform was measured during 5-day trainings; (D-E) In the probe trial, the percentage of time that the mouse spent navigating in the target quadrant and platform crossing times was analyzed. (F) The percentage of perfect alternations (alternation rate) in the Y maze was calculated. (G) distance traveled in the open field test (OFT). All data are shown as mean ± SEM.

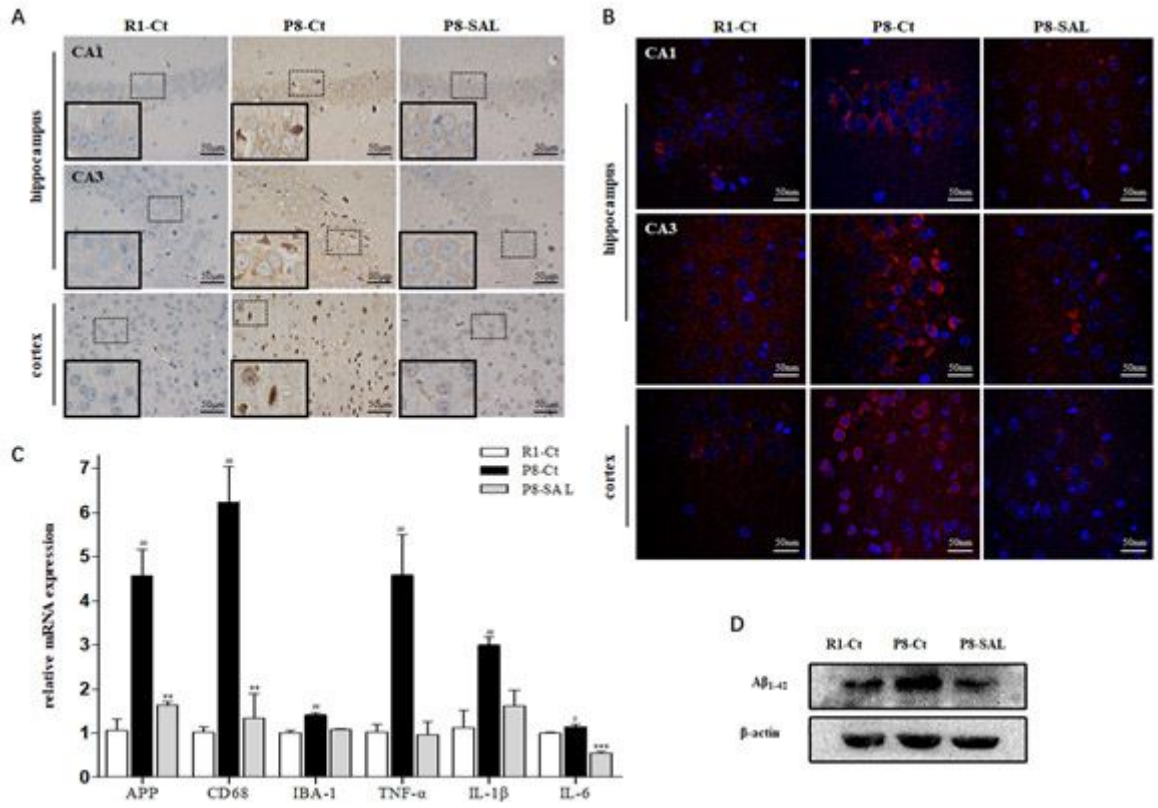

Figure 2

Effect of SAL on neurodegeneration and neuroinflammation in SAMP8. (A) Immunohistochemical staining of Aβ1-42 in hippocampus and cortex for each group (magnification 400X). Dotted box is enlarged in the inset. (B) Representative images of Immunofluorescence analysis using antibody CD68(red) and DAPI (blue) in the cerebral hippocampus (CA1 and CA3 regions) and cortex (magnification 400X). (C) The mRNA levels of APP, CD68, IBA-1,IL-1β, IL-6, TNF-αwere determined by real-time PCR. All data are shown as mean ± SEM. (D)Western blot analysis of Aβ1-42 expression in hippocampus.

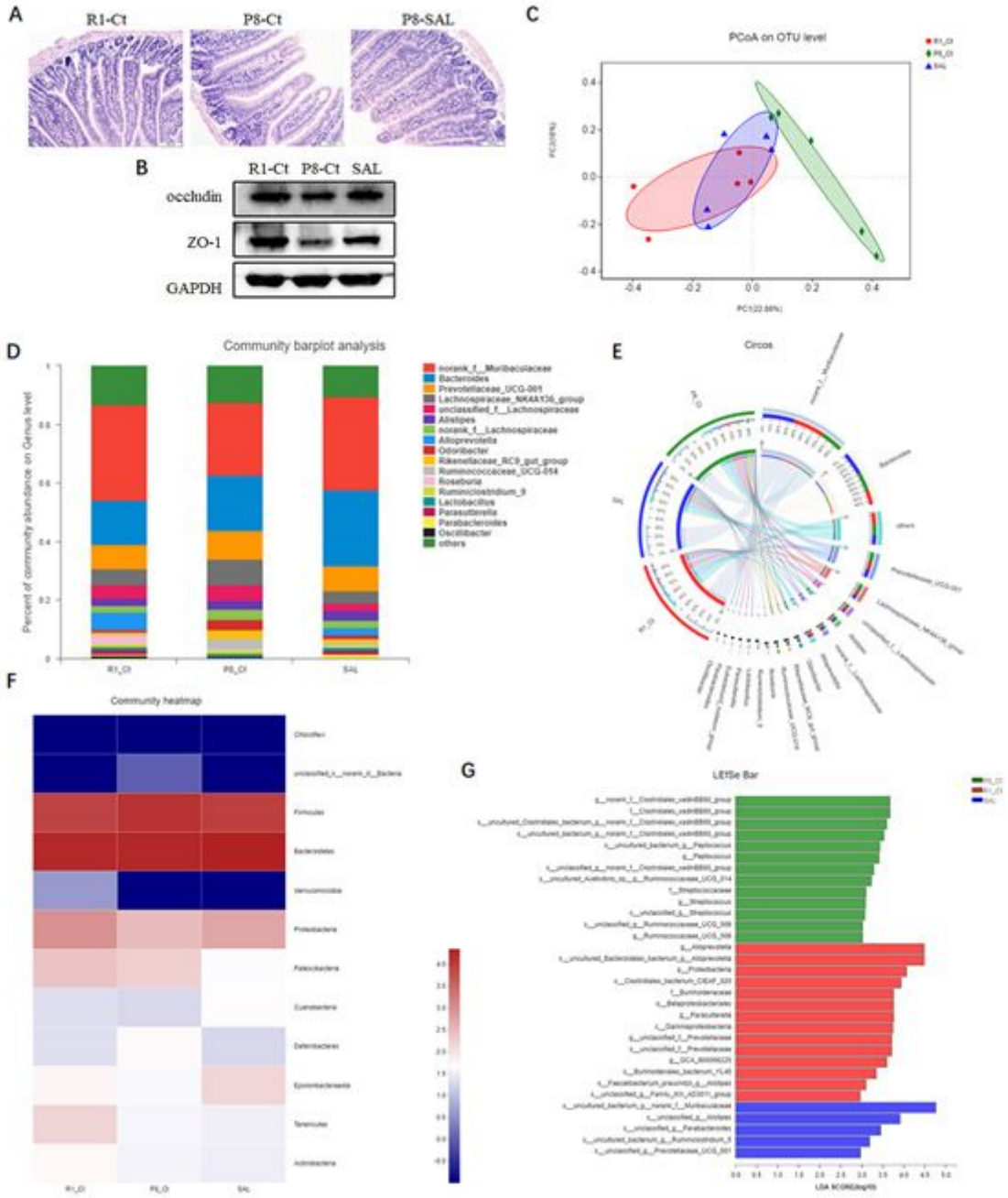

Figure 3

Effect of SAL on intestinal barrier and gut microbiota in SAMP8. (A) HE staining of mice intestinal tissues (scale bar = 100 μm). (B)western blot analysis of ZO-1 and occludin in the intestine. (C)PCoA plots of Bray-Curtis distance on OTU level. (D)Barplot analysis and (E)circos diagram of the relative abundance on genus level in the community. All that less than 0.01(1%) are summed into the category “others”. (F)Heatmap of microbial community abundance profiles at the phylum level. Top 50 species by total abundance. (G) The results of LEfSe analysis (LDA > 2), from the phylum to the species level.

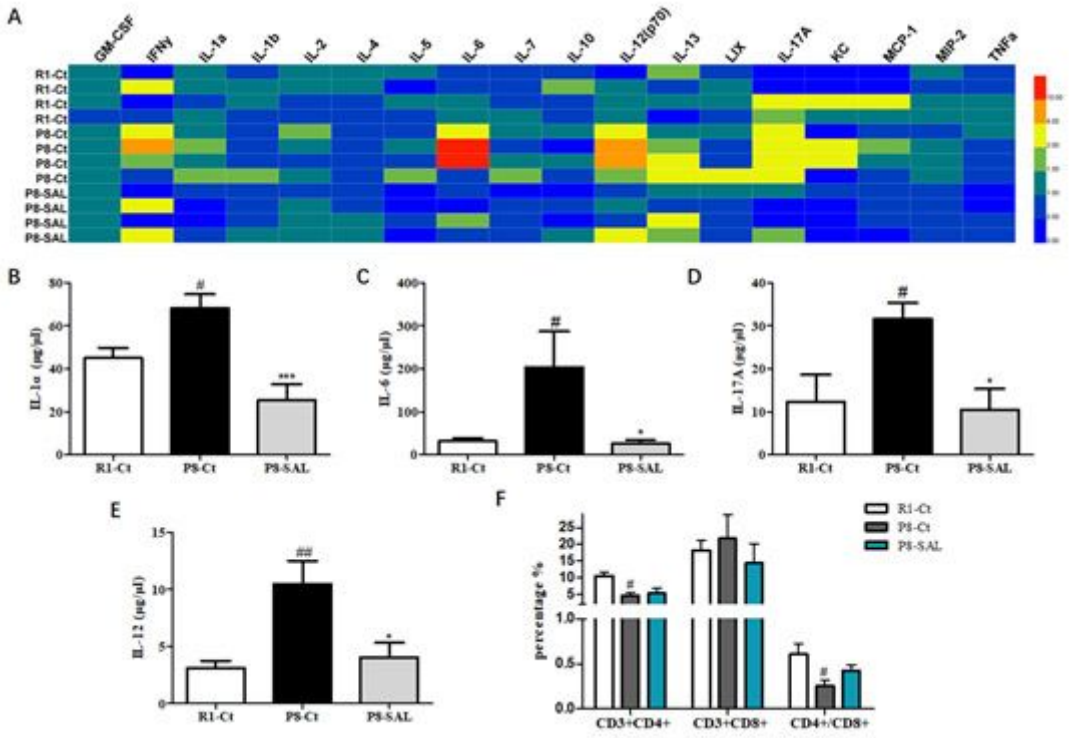

Figure 4

Effect of SAL on peripheral inflammation in SAMP8. (A) Heatmap of 18 serum cytokines/chemokines, detected by Mouse High Sensitivity T Cell Magnetic Bead Panel. Quantitation of (B) IL-1α, (C) IL-6, (D) IL-12 and (E) IL-17A. (F) Spleen index was calculated as spleen weight (g)/mouse weight (g). (G) Flow cytometry results, including proportions of CD3+CD4+ and CD3+CD8+ cells, and the ratio of CD4+/CD8+ in spleen lymphocytes. Bars represent mean ± SE for each group(n=3).

Supplementary Files

This is a list of supplementary files associated with this preprint. Click to download.

- graphabstract.docx
- SupplementaryMaterials.docx